Dynamics of High-Barrier Surface Reactions: Laser-Assisted Associative Desorption of N_2 from Ru(0001)

L. Diekhöner,[1] H. Mortensen,[1] A. Baurichter,[1] A. C. Luntz,[1] and B. Hammer[2]

[1]*Fysisk Institut, SDU-Odense Universitet, Campusvej 55, DK-5230 Odense M, Denmark*
[2]*Institute of Physics, Aalborg University, Pontoppidanstræde 103, DK-9220 Aalborg Øst, Denmark*
(Received 22 December 1999)

We have determined the dynamics and energetics of associative desorption of N_2 from Ru(0001) using both an experimental technique, laser-assisted associative desorption, and density functional calculations. These show that N_2 is preferentially desorbed into very high vibrational states and that the barriers between gas phase N_2 and adsorbed N atoms increase from 2 to >3 eV with increasing N coverage on the surface. This experimental technique is found to be quite insensitive to low barrier steps and defects which complicate interpretations from other methods of studying high-barrier surface reactions.

It is well recognized that the activated dissociation of simple gas phase molecules at metal surfaces is often the rate-limiting step in many industrially important catalytic processes. This has stimulated much experimental and theoretical work over the past several decades in the kinetics and dynamics of activated dissociative chemisorption. For example, high-pressure experiments can in principle determine the activation energy for dissociation, although being very sensitive to the presence of defects and steps, especially when barriers are high [1,2]. Similarly, molecular beam techniques have clarified some dynamical issues in activated dissociative chemisorption, e.g., the role of precursors versus direct mechanisms, the role of translational versus vibrational energy in promoting dissociation, etc. When dissociation barriers are very high, however, or principally along a vibrational coordinate, molecular beam techniques may be difficult to interpret. The dynamics of dissociative chemisorption has recently been inferred by laser state-resolved measurements of the time-reversed process, i.e., associative desorption, and by then invoking detailed balance [3–5].

In this Letter, we describe a technique which we term laser-assisted associative desorption (LAAD) that provides great insight into the dynamics of associative desorption and its time-reversed process, dissociative chemisorption. This technique does *not* require laser state-resolved detection and is generally applicable, regardless of the height of the barrier or whether it is along a translational or vibrational coordinate. Furthermore, it is quite insensitive to the presence of defects and steps on the surface and can be used over a wide range of adsorbate coverages. As an example of the power of this LAAD technique, we present a dynamical study of the interaction of N_2 with a Ru(0001) surface. We will show that these experimental results are in excellent agreement in detail with density functional theory (DFT).

The interaction of N_2 and N with Ru(0001) has attracted much attention recently due to the possible role of supported Ru as an end catalyst for NH_3 synthesis. The rate-limiting step is the dissociative chemisorption of N_2. On Ru(0001), dissociation is strongly activated. Low coverage states of N adsorbed on Ru(0001) [$\theta_N = 0.25$ and 0.33 ML (monolayer)] are well known and have been characterized experimentally [6] and theoretically [7,8]. It has recently been shown that a series of higher coverage states are also formed in addition by exposure to a N atom beam, ultimately saturating at a coverage $\theta_N \sim 1$ ML [9]. By comparing with DFT calculations of the binding energies of N on Ru(0001) as a function of N coverage it was suggested that all states for $\theta_N \gtrsim 0.5$ were only *metastable,* with lifetimes determined by the barrier between gas phase N_2 and the adsorbed N.

The essence of the LAAD application described here is to measure the translational energy distribution of N_2 formed by associative desorption from a Ru(0001) surface following a laser induced temperature jump. Neglecting tunneling and coupling to the lattice, we anticipate that the total energy of the desorbing N_2 is given approximately by the barrier height relative to the N_2 + Ru(0001) asymptote. Because both internal and translational excitations are anticipated in this associative desorption [3,5], the overall measured translational energy distribution represents a sum of the translational distributions for each internal state weighted by the population of that state. If the vibrational state $\nu = 0$ is sufficiently populated to be detected, then the translational energy observed for this state corresponds approximately to the barrier height, since rotational excitation is small [5].

After exposure of a Ru(0001) crystal to a N atom beam to produce a N atom coverage θ_N [9], LAAD experiments were performed by irradiating the surface with a pulsed Alexandrite laser from Light Age Inc. with a wavelength of 750 nm and duration 130 ns. Since the wavelength is in the near IR, laser induced photochemistry is highly unlikely. Thus, the resulting excitation of the surface is well described as a thermally induced temperature jump (T-jump). The surface temperature T_s is shown to basically follow the laser temporal profile [10].

Since the T-jump and resulting N_2 desorption occur only for ca. 100 ns, time of flight techniques (TOF) can be used to measure the translational energy distribution. The desorbing N_2 was detected normal to the surface with a differentially pumped quadrupole mass spectrometer. To determine absolute TOF from the surface to the detector, extensive calibrations of the TOF delays through the mass spectrometer were necessary and a convolution over finite ionizer length performed in the analysis. Most LAAD experiments were performed with N^{15}, due to a lower background at mass 30. No isotope effect was observed. Many checks were performed to make sure that no laser damage [10] occurred on the surface or affected the TOF results in any way.

An example of the TOF distribution for N_2^{15} obtained by LAAD for an initial coverage $\theta_N = 0.6$ is given in Fig. 1, representing an average of 1800 laser shots spread over 60 spatial spots on the surface. The yield of N_2 produced per laser shot is very small ($\ll 10^{-3}$ ML); therefore the TOF produced by many laser shots could be averaged without changing θ_N significantly. Since the time window in the TOF data taking was small (320 ns), raw TOF data were smoothed using a five point Savitzky-Golay algorithm. The corresponding translational energy is given at the top of Fig. 1. It is evident that the overall TOF distribution consists of a series of partially overlapping narrower peaks. We assign these individual peaks to desorption of N_2^{15} in different vibrational states ν, with the higher vibrational states occurring at longer TOF. Assuming $\nu = 0$ is sufficiently populated to be observed in the TOF, then the high energy threshold corresponds approximately to the barrier height V^*.

In order to test this interpretation more quantitatively, we have developed the following simple model for associative
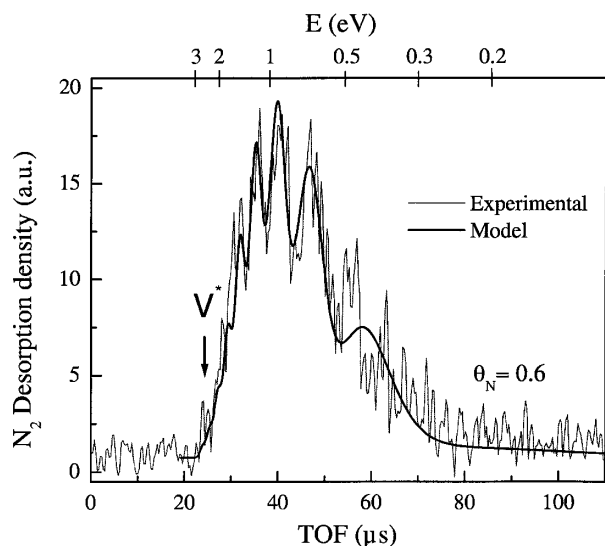
FIG. 1. TOF distribution for laser-assisted associative desorption of N_2^{15} following a T-jump to 875 K. The translational energy is indicated on the top axis. The energy of the barrier V^* (relative to gas phase N_2) is marked with an arrow.

desorption of N_2. Conservation of the total energy from the transition state into the desorbed product implies approximately that $E_{tot} \approx V^* + k_B T_s = E + \varepsilon_\nu + \delta$, where E is the translational energy, ε_ν is the zero point corrected vibrational energy, and δ reflects the energy loss or gain from translation and vibration to modes of the lattice or other N_2 modes (rotation) during the desorption event. We assume that δ is given by a Gaussian distribution of width W and with $\langle \delta \rangle \approx 0$. The total desorption probability is a sum of probabilities from individual vibrational states centered at translational energies $E_0(\nu) = E_{tot} - \eta_\nu \varepsilon_\nu$, where $\eta_\nu \varepsilon_\nu$ is the lowering of the effective barrier in producing state ν (η_ν is the vibrational efficacy). Thermally averaging this desorption density leads to

$$D_\theta(E, T_s) \propto \sqrt{E} \exp\left(-\frac{E}{k_B T_s}\right) \sum_\nu \exp\left(-\frac{\varepsilon_\nu}{k_B T_s}\right)$$
$$\times \left\{ P(\nu) \left[1 + \mathrm{erf}\left(\frac{E - E_0(\nu)}{W} \right) \right] \right\}. \quad (1)$$

$P(\nu)$ is the relative probability of desorption into state ν. Identifying the terms inside the { } as the sticking function, $S_0(E, \nu)$, for dissociative chemisorption of the vibrational state ν, leads to a form for $D_\theta(E, T_s)$ known from detailed balance arguments [11]. Employing that the observed TOF desorption density is given as $D_\theta(t) \propto (1/t^2) D_\theta(E, T_s)$, Eq. (1) was used to fit the data.

We have used the approach of information theory [12] to reduce the assignment of values to $P(\nu)$ to one parameter: the so-called vibrational "surprisal" λ describing the dynamical constraints. This approach has been very successful in describing detailed state-resolved atom-molecule collision experiments in the gas phase [12]. Application of information theory to associative desorption of N_2 gives $P(\nu) = P^0(\nu) \exp(-\lambda f_\nu)/Q$, where $f_\nu \approx \varepsilon_\nu/E_{tot}$ and Q is a normalization constant. $P^0(\nu) = 2.5(1 - f_\nu)^{3/2} E_{tot}^{-1}$ is the statistical (microcanonical) expectation to produce the vibrational state ν given the total energy E_{tot} available for desorption. We assume that $\eta_\nu = 1$ since the low ν states are separated in translational energy by ε_ν. This assumption is consistent with a barrier strongly in the vibrational coordinate.

Given the above model, $D_\theta(E, T_s)$ and hence the TOF distribution are determined by only three parameters, V^*, λ, and W, as well as T_s [13]. $T_s = 875$ K for Fig. 1. The three parameters in the model are well constrained by the observed TOF distribution. A value of $W \approx 0.1$ eV is necessary from the partial resolution of the individual ν states in the TOF. λ must be a large negative number to make $P(\nu)$ peak at higher ν, i.e., to describe a strong vibrational inversion. V^* is chosen so that the high kinetic energy threshold in the model agrees with the experimental TOF. The theoretical curve in Fig. 1 is produced with the "best fit" parameters $W = 0.09$ eV, $\lambda = -12$, and $V^* = 2.5$ eV. The actual labeling of the ν for each peak is not possible. This produces some uncertainty in the determination of V^*. In this fit, we have assumed that

desorption of $\nu = 0$ defines the threshold. If $\lambda \ll -12$ so that $\nu = 0$ is not sufficiently populated to be observed in desorption, equally good fits to the data are obtained with V^* correspondingly higher. However, when $\lambda \gg -12$, agreement with the experiment is decidedly worse. Thus we interpret the experiment to say $V^* \geq 2.5$ eV. Clearly the signal-to-noise ratio (S/N) also limits the ability to establish this lower bound, perhaps by an additional uncertainty of ± 0.2 eV.

The overall agreement between the model and experiment in Fig. 1 is excellent and clearly demonstrates that the spacing between the partially resolved peaks is due to vibrational excitation. We believe the disagreement in the peak observed at 55 μs in the TOF (predicted at 58 μs) is due to a breakdown of the assumption $\eta_\nu = 1$ near the top of the barrier. Our measurements are fully consistent with simple adiabatic dynamics anticipated from the *ab initio* potential energy surface from DFT calculations [5,8], where a high barrier was found to lie almost exclusively along the vibrational coordinate.

State-resolved experiments of associative desorption of N_2 from Ru(0001) [5] showed a population inversion between $\nu = 1$ and $\nu = 0$, consistent with $P(\nu)$ peaking for $\nu \geq 7$ as observed by us. Murphy *et al.* observed desorption from an individual vibrational-rotational state peaking at low (ca. thermal) translational energies, but also a tailing to much higher translational energies, in qualitative disagreement with us. It has been suggested [1] that these results are strongly influenced by desorption from steps or defects. Since our results are fully consistent with anticipated dynamics on the majority terrace sites, this implies that the LAAD measurements are quite immune to the presence of minority low barrier steps and defects. The central reason for this is that during a T-jump of only 100 ns adsorbed N does not have sufficient time to diffuse to the steps or defects which otherwise might dominate associative desorption.

LAAD measurements as a function of θ_N are given in Fig. 2. There is a decided shift in the TOF distribution to higher translational energies with increasing θ_N, and this is taken as evidence for an increase of the barrier with θ_N. Although vibrational resolution is apparent at higher θ_N, it is not observed for the lower θ_N. The principal reason for this is that, because of the lower desorption yield at lower θ_N, averaging TOF experiments for several independent N exposures in addition to averaging each exposure over the different spatial spots was necessary to achieve S/N. Because each N exposure produced a slightly different θ_N, the vibrational resolution was washed out due to the shift of V^* with θ_N. Assuming that $\lambda \approx -12$ for all θ_N, application of the model outlined previously gives the lower bounds to barriers $V^*(\theta_N)$ marked in Fig. 2 as arrows. The justification for assuming a constant λ with θ_N is that the N-N bond length at the transition state was nearly independent of θ_N in the DFT calculations. The barriers are given in Table I and are seen to increase from approximately 2 eV at low θ_N to 3 eV at the highest θ_N. A simi-
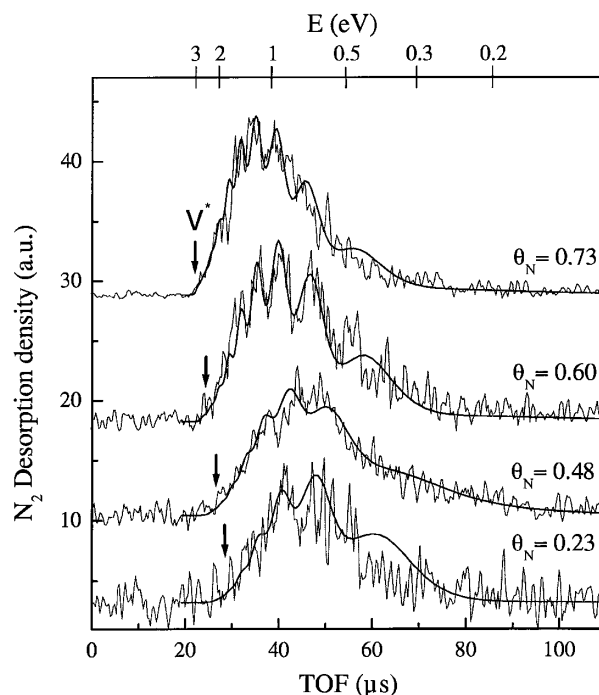
FIG. 2.   TOF distributions for LAAD of N_2^{15} as a function of N coverage. The energies of the barriers V^* (relative to gas phase N_2) are marked with arrows. LAAD occurred at 800, 875, 1000, and 1700 K for $\theta_N = 0.73$, 0.60, 0.48, and 0.23 ML, respectively.

lar increase in barrier with θ_N was indirectly inferred from thermal desorption measurements as a function of coverage [9].

In order to understand the origin of the barrier increase with θ_N we have performed DFT calculations of the transition from adsorbed N to gas phase N_2 as a function of θ_N. Figure 3 shows the results of these calculations with respect to $N_2(g)$ and clean Ru(0001). Four consecutive N_2 desorption events (*A*, *B*, *C*, and *D*) are described in a $c(4 \times 4)$ surface supercell which initially accommodates eight N atoms in its eight hcp sites [14]. The surface supercell is repeated periodically, whereby we effectively investigate N_2 desorption in the range $0.25 \leq \theta_N \leq 1$.

In Fig. 3, the potential energy levels of the various stages of the adiabatic N_2 desorption events are indicated by open squares (most stable configuration of the surface at a given coverage), asterisks (transition state for the association of two N atoms from neighboring hcp sites), and solid squares (metastable surface configuration including a N divacancy where the desorption took place). Since the time scale of the LAAD experiment is very short compared to annihilation of the divacancy, the adsorption barrier, E_a, is

TABLE I.   Measured (V^*) and calculated (E_a) values of the coverage dependence of the energy barrier.

θ_N	ML	0.23	0.32	0.48	0.60	0.73	$\cdots$
V^*	eV	1.8	2.0	2.1	2.5	2.8	$\cdots$
θ_N	ML	0.25	$\cdots$	0.50	$\cdots$	0.75	1.00
E_a	eV	2.1	$\cdots$	2.2	$\cdots$	3.5	4.8
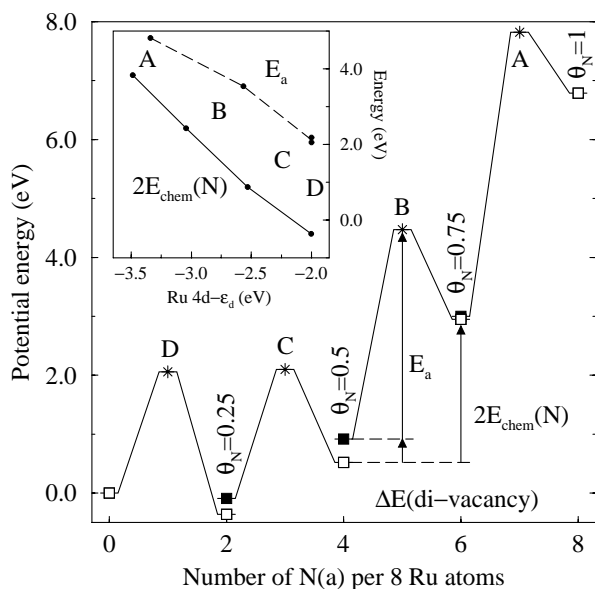
FIG. 3. Calculated potential energy diagram for desorption of N_2 from Ru(0001)-$c(4 \times 4)$ initially at $\theta_N = 1$. The inset shows (twice) the differential chemisorption energy of N, $E_{chem}(N)$, and the energy barrier for dissociation at a divacancy as a function of the Ru $4d$ band center, ε_d.

evaluated from the level including such a divacancy to the level of the transition state in the case of the desorption events A, B, and C. Assigning θ_N for each calculated E_a corresponding to the N coverage in the supercell before the desorption, we obtain the values given in Table I. Judging from the table, there is excellent agreement between these DFT calculations and the values obtained by the LAAD experiment, both in the magnitude of the barrier and in its coverage dependence.

It has previously been demonstrated that there is a strong correlation of both surface adsorption energies and barriers to dissociation on transition metals with the center of the metal d bands [15]. In the inset of Fig. 3 we show for the first time that such a correlation also exists for the coverage dependence of differential chemisorption energies and energy barriers. The Ru $4d$-band centers ε_d as a function of θ_N are constructed as geometrical means of the first moments of the $4d$-projected density of states at Ru sites neighboring the reaction site. The ε_d at these sites decrease with θ_N, because the Ru atoms have their electronic $4d$ states shifted down compared to the clean surface value as a consequence of the bonding to the preadsorbed N. Both the atomic chemisorption energies and the energy barriers increase with the decrease in ε_d because the lower in energy the Ru $4d$ electrons are, the less they are capable of interacting chemically with the electronic levels on the adsorbed N as well as on the transition state [15].

In summary, we have described the application of LAAD to determine both the dynamics and energetics of N_2 associative desorption from Ru(0001). This technique seems rather immune to complications caused by low-

barrier minority sites. We find that N_2 is preferentially produced in high vibrational states and that the barrier between gas phase N_2 and the adsorbed N atoms increases substantially with θ_N. Both the energetics and dynamics are in excellent agreement with DFT calculations for the process. The DFT calculations show that the origin of this increase in barrier with coverage can be understood in terms of coverage dependent shifts of the Ru $4d$-band centers.

The authors acknowledge the Danish Research Council for support of this work under Grants No. 9601724, No. 9800425, and No. 9803041.

[1] S. Dahl, A. Logadottir, R. C. Egeberg, J. H. Larsen, I. Chorkendorff, E. Törnqvist, and J. K. Nørskov, Phys. Rev. Lett. **83**, 1814 (1999).

[2] B. Hammer, Phys. Rev. Lett. **83**, 3681 (1999).

[3] H. A. Michelsen, C. T. Rettner, and D. J. Auerbach, Phys. Rev. Lett. **69**, 2678 (1992).

[4] M. J. Murphy and A. Hodgson, J. Chem. Phys. **108**, 4199 (1998).

[5] M. J. Murphy, J. F. Skelly, A. Hodgson, and B. Hammer, J. Chem. Phys. **110**, 6954 (1999).

[6] K. Jacobi, H. Dietrich, and G. Ertl, Appl. Surf. Sci **121**, 558 (1997).

[7] S. Schwegmann, A. P. Seitsonen, H. Dietrich, H. Bludau, H. Over, K. Jacobi, and G. Ertl, Chem. Phys. Lett. **264**, 680 (1997).

[8] J. J. Mortensen, Y. Morikawa, B. Hammer, and J. K. Nørskov, J. Catal. **169**, 85 (1997).

[9] L. Diekhöner, A. Baurichter, H. Mortensen, and A. C. Luntz, J. Chem. Phys. **112**, 2507 (2000); L. Diekhöner, H. Mortensen, A. Baurichter, and A. C. Luntz, J. Vac. Sci. Technol. (to be published).

[10] J. F. Ready, *Effects of High-Power Laser Radiation* (Academic Press, New York, 1971); A. M. Prokhorov, V. I. Konov, I. Ursu, and I. N. Mihailescu, *Laser Heating of Metals* (Hilger, Bristol, 1990).

[11] H. A. Michelsen and D. J. Auerbach, J. Chem. Phys. **94**, 7502 (1991).

[12] R. D. Levine, in *Annual Review of Physical Chemistry,* edited by B. S. Rabinovitch, J. M. Schurr, and H. L. Strauss (Annual Reviews, Palo Alto, 1978), Vol. 29, p. 59; R. B. Bernstein, *Chemical Dynamics Via Molecular Beam and Laser Techniques* (Oxford University Press, New York, 1982).

[13] T_s is time dependent, but 90% of the desorption occurs within 100 K of the peak. We thus assume T_s is constant and estimate this from CO laser desorbed, with TOF's well described by Boltzmann distributions at $2k_B T_s$.

[14] The RPBE XC functional [B. Hammer *et al.,* Phys. Rev. B **59**, 7413 (1999)] is used. Other calculational details are as in Ref. [2].

[15] B. Hammer and J. K. Nørskov, in *Chemisorption and Reactivity on Supported Clusters and Thin Films,* edited by R. M. Lambert and G. Pacchioni (Kluwer Academic Publishers, The Netherlands, 1997), pp. 285–351.